Calculations executed for the 3-bladed rotor of the VIRYA-3B3 windmill (λ_d = 6.5, wooden blades)

ing. A. Kragten

February 2012
reviewed November 2018

KD 484

It is allowed to copy this report for private use. It is allowed to use the described rotor but the rotor is not yet tested. The rotor should not be used on a wind turbine without a proper safety system. Kragten Design accepts no responsibility for possible failures.

Engineering office Kragten Design
Populierenlaan 51
5492 SG Sint-Oedenrode
The Netherlands
telephone: +31 413 475770
e-mail: info@kdwindturbines.nl
website: www.kdwindturbines.nl

Contains page

1 Introduction

The VIRYA-3B3 windmill is developed for 24 V or 12 V battery charging. The VIRYA-3B3 is meant for use in Western countries but also for use in developing countries if the required stainless steel is available. The VIRYA-3B3 has a 3-bladed rotor with wooden blades. The 3-bladed rotor is an alternative for the 2-bladed rotor with wooden blades of the VIRYA-3. A 3-bladed rotor with wooden blades has been tested for the VIRYA-3.3 windmill for many years. The noise production of a rotor with wooden blades is very low.

The windmill is provided with the so called hinged side vane safety system and has a rated wind speed V_{rated} of about 9.5 m/s. The head and tower geometry is the same as that of the VIRYA-3. The generator is mechanically the same as the generator of the VIRYA-2.68 with stainless steel blades but the original 230/400 V winding is modified into a 115/200 V winding by connecting the first and the second layer in parallel in stead of in series. The winding is rectified in star for 24 V battery charging and in delta for 12 V battery charging.

The generator is based on an asynchronous 3-phase motor of manufacture ROTOR type 5RN90L04V (with lengthened stator iron) for which the short-circuit armature is replaced by an armature provided with permanent magnets. The generator with the original 230/400 V winding has been measured on a test rig of the University of Technology Eindhoven and the test results are given in report KD 78 (ref. 1).

The windmill has a 3 m upper tower section made of 2 ½" gas pipe and a 7 m four legs lower tower section made of angle iron and strip. The lower tower section is build up from two 3.5 m long parts. The lower section is connected to the foundation by hinges.

The battery charge controller and dump load are identical to those of the VIRYA-3.8 windmill.

2 Description of the rotor of the VIRYA-3B3 windmill

The 3-bladed rotor of the VIRYA-3B3 windmill has a diameter D = 3 m and a design tip speed ratio λ_d = 6.5. Advantage of a 3-bladed rotor above a 2-bladed rotor are that the gyroscopic moment in the rotor shaft is not fluctuating and that a 3-bladed rotor is generally judged as more beautiful.

The rotor has blades with a constant chord and blade angle and is provided with a Gö 623 airfoil (or a Gö 711-12 % airfoil) with a chord of 150 mm. A blade is made of a hard wood plank with dimensions of 18 * 150 * 1425 mm. The whole blade length is provided with the Gö 623 airfoil, so including the part where it is clamped. A blade is covered with two layers of epoxy and two layers of aluminium paint to make the wood weather resistant.

The blades are connected to each other by a hub plate which is made of 5 mm stainless steel sheet. The hub plate has three ears with a length of 225 mm and a width of 130 mm The overlap in between blade and hub plate is 150 mm. A blade is connected to the ear of a hub plate by three bolts M10. A stainless steel strip size 2 * 40 * 150 is mounted in between the bolt heads and the back side of the blade to prevent deformation of the wood. Each ear of the hub plate is twisted in between r = 35 mm and r = 75 mm to realize the correct blade setting angle of the blades. One hub plate can be made from a sheet size 5 * 395 * 460 mm. Four hub plates can be laser cut from a sheet size 5 * 460 * 1500 mm. Thirty six hub plates can be laser cut from a 5 mm sheet size 1.5 * 3 m.

The hub is made out of a piece of stainless steel bar with a diameter of 70 mm with a tapered hole in the middle for connection to the generator shaft. The hub plate is connected to the hub using three bolts M10. The hub is connected to the tapered shaft of the generator by one central bolt M10. The rotor is balanced by adding balancing weights at the outer connecting bolts. After balancing, blades hub and balancing weights are market to get the correct blade at the correct ear of the hub plate. The rotor drawing with format A1, has drawing number 1201-01. A photo of the drawing is added in appendix 2.

3 Calculation of the rotor geometry

The rotor geometry is determined using the method and the formulas as given in report KD 35 (ref. 2). This report (KD 484) has its own formula numbering. Substitution of $\lambda_d = 6.5$ and R = 1.5 m in formula (5.1) of KD 35 gives:

$\lambda_{r\,d} = 4.3333 * r$ (-) (1)

Formula's (5.2) and (5.3) of KD 35 stay the same so:

$\beta = \phi - \alpha$ (°) (2)

$\phi = 2/3 \arctan 1 / \lambda_{r\,d}$ (°) (3)

Substitution of B = 3 and c = 0.15 m in formula (5.4) of KD 35 gives:

$C_l = 55.8505\ r\ (1 - \cos\phi)$ (-) (4)

Substitution of V = 5 m/s and c = 0.15 m in formula (5.5) of KD 35 gives:

$R_{e\,r} = 0.50 * 10^5 * \sqrt{(\lambda_{r\,d}^2 + 4/9)}$ (-) (5)

The blade is calculated for eight stations A till H which have a distance of 0.225 m of one to another except for the distance in between stations F, G and H which is 0.15 m. The blade has a constant chord and the calculations therefore correspond to the example as given in chapter 5.4.2 of KD 35. This means that the blade is designed with a low lift coefficient at the tip and with a high lift coefficient at the root. First the theoretical values are determined for C_l, α and β and next β is linearised such that the blade angel is constant and that the linearised values for the outer part of the blade correspond as good as possible with the theoretical values. Next the values for α_{lin}, $C_{l\,lin}$ and $C_d/C_{l\,lin}$ are determined. The result of the calculations is given in table 1. The aerodynamic characteristics of the Gö 623 airfoil are given in chapter 5.5 of KD 35. The Reynolds values for the stations are calculated for a wind speed of 5 m/s because this is a reasonable wind speed for a windmill with a rated wind speed of 9.5 m/s. Those airfoil Reynolds numbers are used which are lying closest to the calculated values. A sketch of the rotor is given in appendix 1.

station	r (m)	λ_{rd} (-)	ϕ (°)	c (m)	$C_{l\,th}$ (-)	$C_{l\,lin}$ (-)	$R_{e\,r} * 10^{-5}$ V = 5 m/s	$R_e * 10^{-5}$ Gö 623	α_{th} (°)	α_{lin} (°)	β_{th} (°)	β_{lin} (°)	$C_d/C_{l\,lin}$ (-)
A	1.5	6.5	5.8	0.15	0.43	0.38	3.27	4.2	-0.7	-1.2	6.5	7.0	0.027
B	1.275	5.525	6.8	0.15	0.51	0.49	2.78	2.3	-0.1	-0.2	6.9	7.0	0.034
C	1.05	4.55	8.3	0.15	0.61	0.63	2.30	2.3	1.0	1.3	7.3	7.0	0.029
D	0.825	3.575	10.4	0.15	0.76	0.80	1.82	2.3	2.8	3.4	7.6	7.0	0.025
E	0.6	2.6	14.0	0.15	1.00	1.05	1.34	1.2	6.4	7.0	7.6	7.0	0.040
F	0.375	1.625	21.1	0.15	1.40	0.85	0.88	1.2	-	14.0	-	7.0	0.025
G	0.225	0.975	30.5	0.15	1.74	-	0.59	1.2	-	23.5	-	7.0	-
H	0.075	0.325	48.0	0.15	1.39	-	0.37	1.2	-	41.0	-	7.0	-

table 1 Calculation of the blade geometry of the VIRYA-3B3 rotor

No value for α_{th} and therefore for β_{th} is found for stations F, G and H because the required C_l value can not be generated. The variation of the theoretical blade angle β_{th} is only little for station A up to E and varies in between 6.5° en 7.6°. Therefore it is allowed to take a constant value of 7° for the whole blade. The strips of the spoke assembly are twisted 7° right hand.

4 Determination of the C_p-λ and the C_q-λ curves

The determination of the C_p-λ and C_q-λ curves is given in chapter 6 of KD 35. The average C_d/C_l ratio for the most important outer part of the blade is about 0.03. Figure 4.7 of KD 35 (for B = 3) en λ_{opt} = 6.5 and C_d/C_l = 0.03 gives $C_{p\ th}$ = 0.44. The blade is stalling at station F and the airfoil is disturbed within station G because of the blade connection. Therefore not the whole blade length k = 1.425 m, but only the part up to 0.075 m outside station F is used for the calculation of the C_p. This gives an effective blade length k' = 1.05 m.
Substitution of $C_{p\ th}$ = 0.44, R = 1.5 m and blade length k = k' = 1.05 m in formula 6.3 of KD 35 gives $C_{p\ max}$ = 0.4. $C_{q\ opt} = C_{p\ max} / \lambda_{opt}$ = 0.4 / 6.5 = 0.0615.
Substitution of $\lambda_{opt} = \lambda_d$ = 6.5 in formula 6.4 of KD 35 gives λ_{unl} = 10.4.
The starting torque coefficient is calculated with formula 6.12 of KD 35 which is given by:

$$C_{q\ start} = 0.75 * B * (R - \tfrac{1}{2}k) * C_l * c * k / \pi R^3 \qquad (-) \qquad (6)$$

The blade angle is 7° for the whole blade. For a non rotating rotor the angle of attack α is therefore 90° - 7° = 83°. The estimated C_l-α curve for large values of α is given as figure 5.10 of KD 35. For α = 83° it can be read that C_l = 0.245. The whole blade is stalling during starting and therefore now the whole blade length k = 1.425 m is taken.
Substitution of B = 3, R = 1.5 m, k = 1.425 m, C_l = 0.245 en c = 0.15 m in formula 6 gives that $C_{q\ start}$ = 0.0088. For the ratio between the starting torque and the optimum torque we find that it is 0.0088 / 0.0615 = 0.143. This is acceptable for a rotor met a design tip speed ratio of 6.5.

The starting wind speed V_{start} of the rotor is calculated with formula 8.6 of KD 35 which is given by:

$$V_{start} = \sqrt{\left(\frac{Q_s}{C_{q\ start} * \tfrac{1}{2}\rho * \pi R^3}\right)} \qquad (m/s) \qquad (7)$$

For the generator, a sticking torque Q_s has been measured of about 0.4 Nm if the shaft is not rotating. Substitution of Q_s = 0.4 Nm, $C_{q\ start}$ = 0.0088, ρ = 1.2 kg/m^3 en R = 1.5 m in formula 7 gives that V_{start} = 2.7 m/s. This is acceptable low for a 3-bladed rotor with a design tip speed ratio of 6.5. Because the generator is rectified in star for 24 V battery charging, the rise of the unloaded generator torque is only little at low rpm. The rise is less than the rise of the Q-n curve of the rotor and therefore the real starting wind speed will be about the same as the calculated value. Rectification in delta is more unfavorable because the unloaded Q-n curve of the generator is rising rather fast as higher harmonic currents can circulate in the winding. This will be verified in chapter 7.

In chapter 6.4 of KD 35 it is explained how rather accurate C_p-λ and C_q-λ curves can be determined if only two points of the C_p-λ curve and one point of the C_q-λ curve are known. The first part of the C_q-λ curve is determined according to KD 35 by drawing a S-shaped line which is horizontal for λ = 0.

Kragten Design developed a method with which the value of C_q for low values of λ can be determined (see report KD 97 ref. 3). With this method, it can be determined that the C_q-λ curve is about straight and horizontal for low values of λ if a Gö 623 airfoil is used. A scale model of a three bladed rotor with constant chord and blade angle and with a design tip speed ratio λ_d = 6 has been measured in the wind tunnel already on 20-11-1980. It has been found that the maximum C_p was more than 0.4 and that the C_q-λ curve for low values of λ was not horizontal but somewhat rising. This effect has been taken into account and the estimated C_p-λ and C_q-λ curves for the VIRYA-3B3 rotor are given in figure 1 and 2.

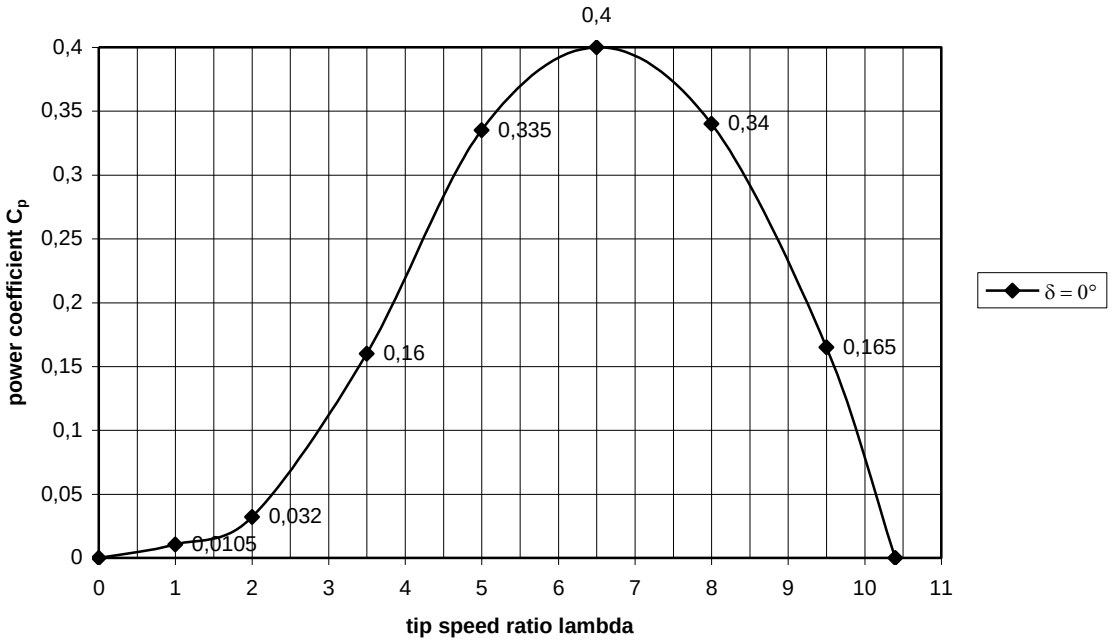

fig. 1 Estimated C_p-λ curve for the VIRYA-3B3 rotor for the wind direction perpendicular to the rotor (δ = 0°)

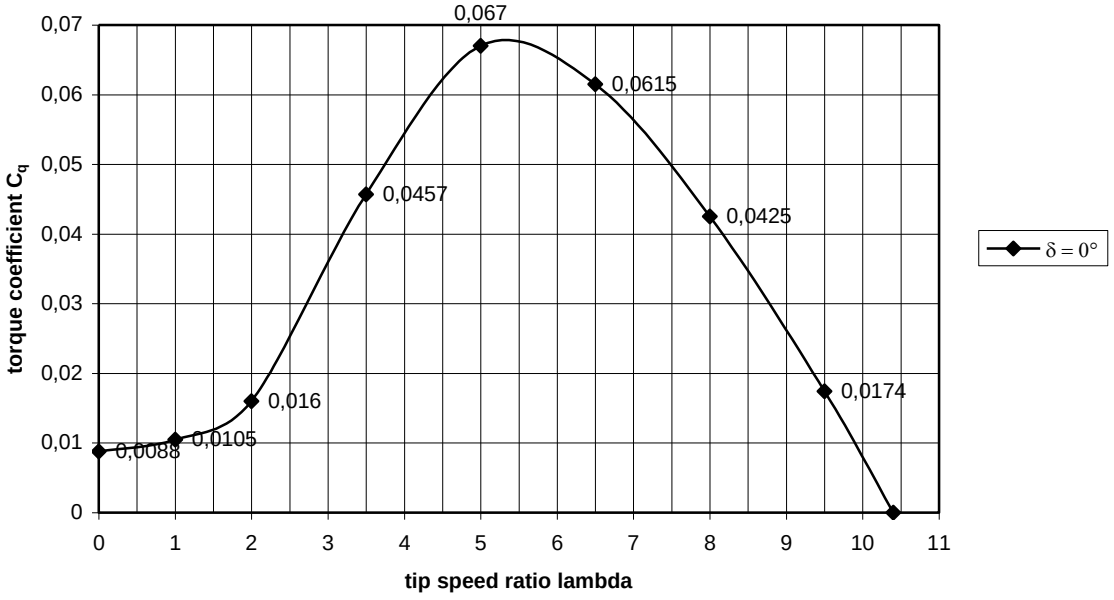

fig. 2 Estimated C_q-λ curve for the VIRYA-3B3 rotor for the wind direction perpendicular to the rotor (δ = 0°)

5 Determination of the P-n curves and the P_{el}-V curve for 26 V star

The determination of the P-n curves of a windmill rotor is described in chapter 8 of KD 35. One needs a C_p-λ curve of the rotor and a δ-V curve of the safety system together with the formulas for the power P and the rotational speed n. The C_p-λ curve is given in figure 1. The δ-V curve of the safety system depends on the vane blade mass per area. The vane blade is made of 9 mm meranti plywood with a density of about $0.6 * 10^3$ kg/m^3. In report KD 213 (ref. 4), a method is given to check the estimated δ-V curve and the estimated δ-V curve of the VIRYA-4.2 windmill is checked as an example. This windmill also has a 9 mm plywood vane blade so the δ-V curves of both windmills will be about the same. The estimated and calculated curves appear to lie close to each other so it is allowed to use the estimated curve. The estimated δ-V curve is given in figure 3. The rated wind speed V_{rated} is about 9.5 m/s.

The head starts to turn away at a wind speed of about 6 m/s. For wind speeds above 9.5 m/s it is supposed that the head turns out of the wind such that the component of the wind speed perpendicular to the rotor plane, is staying constant. The P-n curve for 9.5 m/s will therefore also be valid for wind speeds higher than 9.5 m/s.

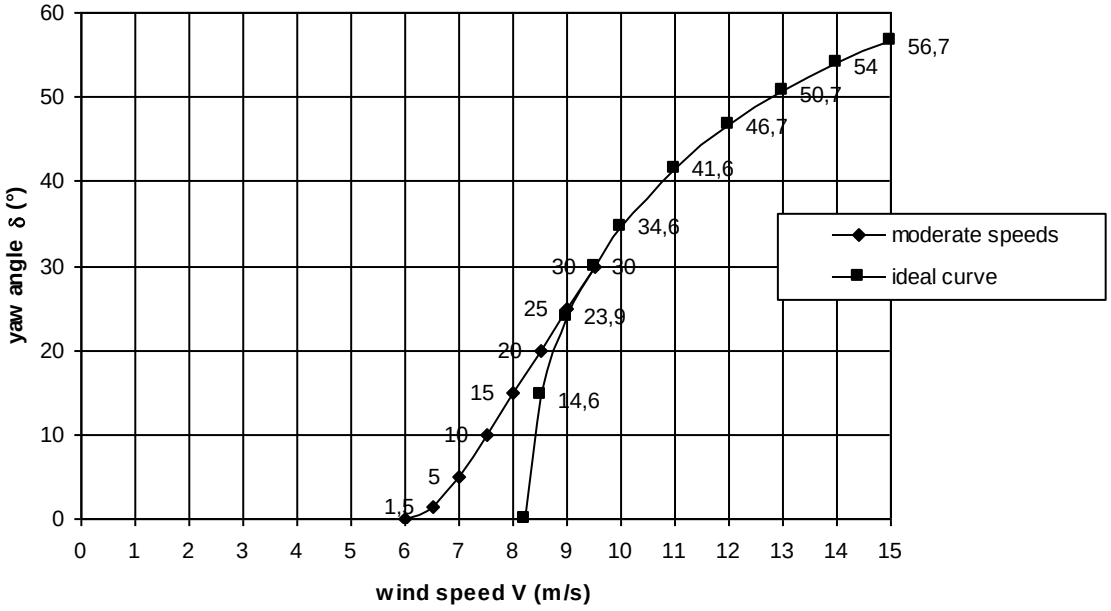

fig. 3 δ-V curve VIRYA-3B3 safety system with V_{rated} = 9.5 m/s

The P-n curves are used to check the matching with the P_{mech}-n curve of the generator for a certain gear ratio i (the VIRYA-3B3 has no gearing so i = 1). Because we are especially interested in the domain around the optimal cubic line and because the P-n curve for low values of λ appears to lie very close to each other, the P-n curves are not determined for low values of λ. The P-n curves are determined for wind the speeds 3, 4, 5, 6, 7, 8 and 9.5 m/s. At high wind speeds the rotor is turned out of the wind by a yaw angle δ and therefore the formulas for P and n are used which are given in chapter 7 of KD 35.

Substitution of R = 1.5 m in formula 7.1 of KD 35 gives:

$$n_\delta = 6.3662 * \lambda * \cos\delta * V \qquad \text{(rpm)} \qquad (8)$$

Substitution of ρ = 1.2 kg / m^3 and R = 1.5 m in formula 7.10 of KD 35 gives:

$$P_\delta = 4.2412 * C_p * \cos^3\delta * V^3 \qquad \text{(W)} \qquad (9)$$

The P-n curves are determined for C_p values belonging to λ is 3.5, 5, 6.5, 8, 9.5 and 10.4 (see figure 1). For a certain wind speed, for instance V = 3 m/s, related values of C_p and λ are substituted in formula 8 and 9 and this gives the P-n curve for that wind speed. For the higher wind speeds the yaw angle as given by figure 3, is taken into account. The result of the calculations is given in table 2.

		V = 3 m/s δ = 0°		V = 4 m/s δ = 0°		V = 5 m/s δ = 0°		V = 6 m/s δ = 0°		V = 7 m/s δ = 5°		V = 8 m/s δ = 15°		V = 9.5 m/s δ = 30°	
λ (-)	C_p (-)	n (rpm)	P (W)	n (rpm)	P (W)	n (rpm)	P (W)	n (rpm)	P (W)	n_δ (rpm)	P_δ (W)	n_δ (rpm)	P_δ (W)	n_δ (rpm)	P_δ (W)
3.5	0.16	66.8	18.3	89.1	43.4	111.4	84.8	133.7	146.6	155.4	230.1	172.2	313.1	183.3	377.9
5	0.335	95.5	38.4	127.3	90.9	159.2	177.6	191.0	306.9	222.0	481.8	246.0	656.6	261.9	791.2
6.5	0.4	124.1	45.8	165.5	108.6	206.9	212.1	248.3	366.4	288.6	575.3	319.8	782.8	340.4	944.7
8	0.34	152.8	38.9	203.7	92.3	254.6	180.3	305.6	311.5	355.2	489.0	393.6	665.4	419.0	803.0
9.5	0.165	181.4	18.9	241.9	44.8	302.4	87.5	362.9	151.2	421.7	237.3	467.3	322.9	497.6	389.7
10.4	0	198.6	0	264.8	0	331.0	0	397.3	0	461.7	0	511.6	0	544.7	0

table 2 Calculated values of n and P as a function of λ and V for the VIRYA-3B3 rotor

The calculated values for n and P are plotted in figure 4. For charging of a 24 V battery, the original 230/400 V winding has to be modified into a 115/200 V winding. How this is done is explained in report KD 341 (ref. 5). The winding has to be rectified in star for 24 V battery charging. Rectification of 3-phase generators is explained in report KD 340 (ref. 6). The generator has been measured for the original 230/400 V winding for 52 V star. All the characteristics for the original winding for 52 V star will be the same as the characteristics for the modified 115/200 V winding for 26 V star. The P_{mech}-n and P_{el}-n curves of the generator for 26 V star, for the modified 115/200 V winding, are also plotted in figure 4. A voltage of 26 V is the average charging voltage for a 24 V battery.

The generator has been measured for short-circuit in delta and for short-circuit in star. Short-circuited in delta is advised because the maximum torque level for short-circuit in delta is higher than for short-circuit in star. Short-circuit in delta is identical to short-circuit in star if the star point is short-circuited too. The P-n curves for short-circuit in delta and for short-circuit in star are also plotted in figure 4.

The point of intersection of the P_{mech}-n curve of the generator with the P-n curve of the rotor for a certain wind speed, gives the working point for that wind speed. The electrical power P_{el} for that wind speed is found by going down vertically from the working point up to the point of intersection with the P_{el}-n curve. The values of P_{el} found this way for all wind speeds, are plotted in the P_{el}-V curve (see figure 5). The charging voltage at high powers will be somewhat higher than the average charging voltage of 26 V and therefore the generator efficiency will be somewhat higher too. This results in a somewhat higher electrical power. The P_{el}-V curve is corrected for this effect for high wind speeds.

The matching of rotor and generator is very good because the P_{mech}-n curve of the generator is lying close to the optimum cubic line for wind speeds in between 4 and 9.5 m/s. In the P_{el}-V curve it can be seen that the maximum power is 500 W and that supply of power starts already at a wind speed of 2.7 m/s ($V_{cut\ in}$ = 2.7 m/s). This is rather low and therefore the windmill can be used in regions with low wind speeds. In chapter 4 it was calculated that V_{start} = 2.7 m/s so there is no hysteresis in the P_{el}-V curve.

The P-n curve for short-circuit in delta is lying left from the P-n curve of the rotor for V = 9.5 m/s and higher. This means that the rotor will slow down to almost stand still for every wind speed if short-circuit in delta is made. The P-n curve for short-circuit in star is also lying left from the P-n curve of the rotor for V = 9.5 m/s and higher but the distance in between both curves is little. So making short-circuit in star to stop the rotor is not advised because, at high wind speeds, it may take a long time for the rotor to stop and the winding may burn in the meantime. Short-circuit in star is the same as short-circuit in delta if the star point is short-circuited too.

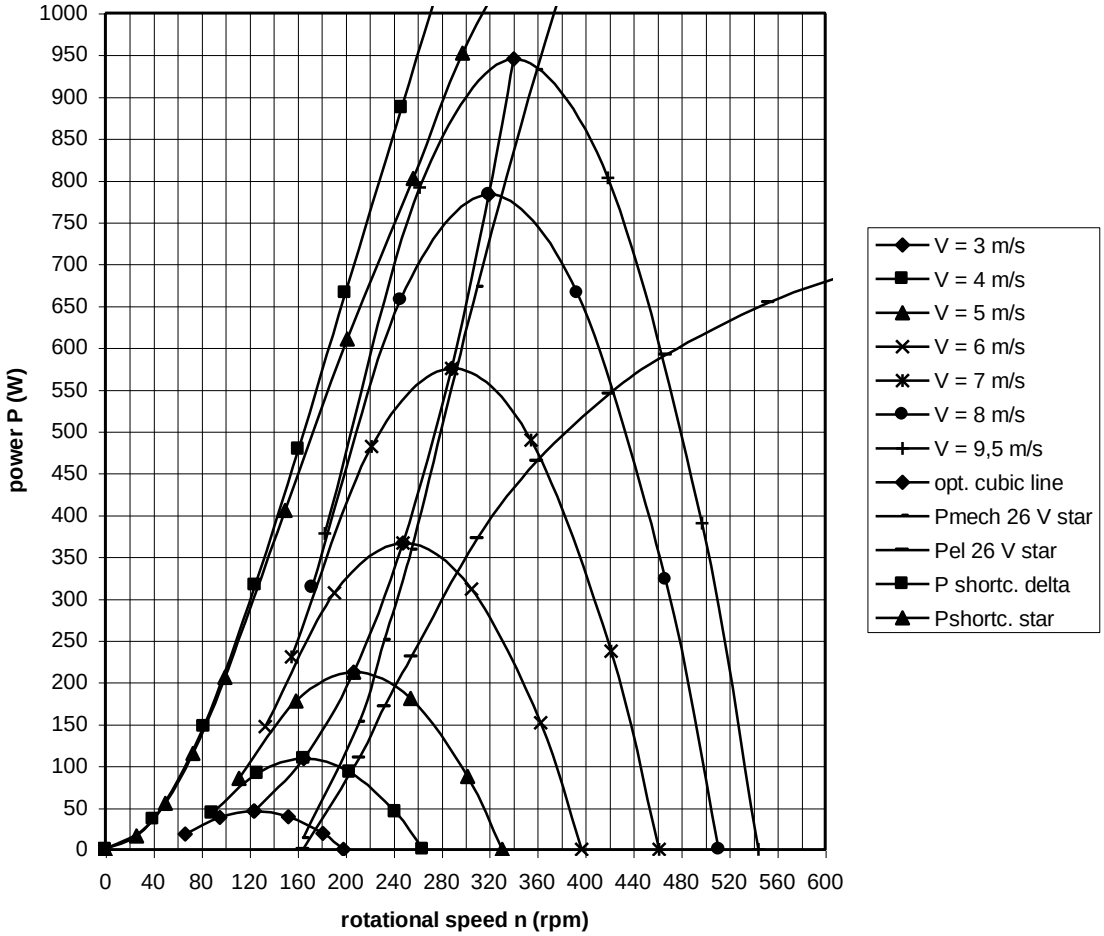

fig. 4 P-n curves of the VIRYA-3B3 rotor for V_{rated} = 9.5 m/s, optimum cubic line, P_{mech}-n and P_{el}-n curves of the generator with modified 115/200 V winding for 26 V star and P-n curves of the generator for short-circuit in delta and star.

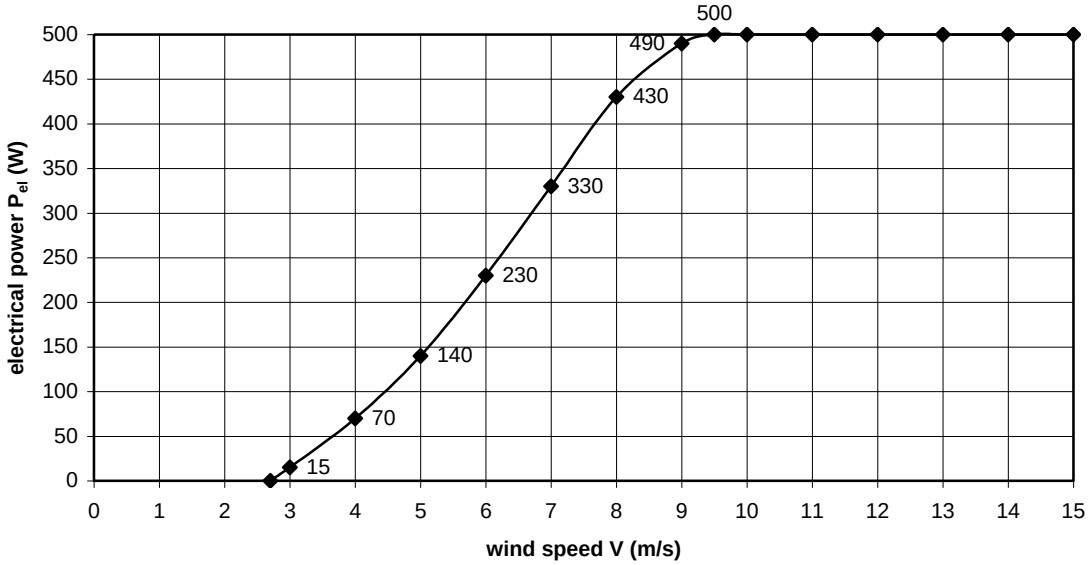

fig. 5 P_{el}-V curve of the VIRYA-3B3 windmill for 24 V battery charging for a modified 115/200 V winding and rectification in star

The same P_{el}-V curve will be found is the VIRYA-3B3 is used for 48 V battery charging with the original 230/400 V winding.

6 Determination of the P-n curves and the P_{el}-V curve for 13 V delta

If there is a need for 12 V battery charging in stead of 24 V battery charging, it might be possible to use the modified 115/200 V winding with rectification in delta. The characteristics for 26 V delta for the original 230/400 V winding are given in report KD 78 (ref. 1). The characteristics for the modified 115/200 V winding will be the same for 13 V delta. Figure 4 is now copied as figure 6 but the curves for 26 V star are replaced by the curves for 13 V delta (13 V is the average charging voltage for a 12 V battery).

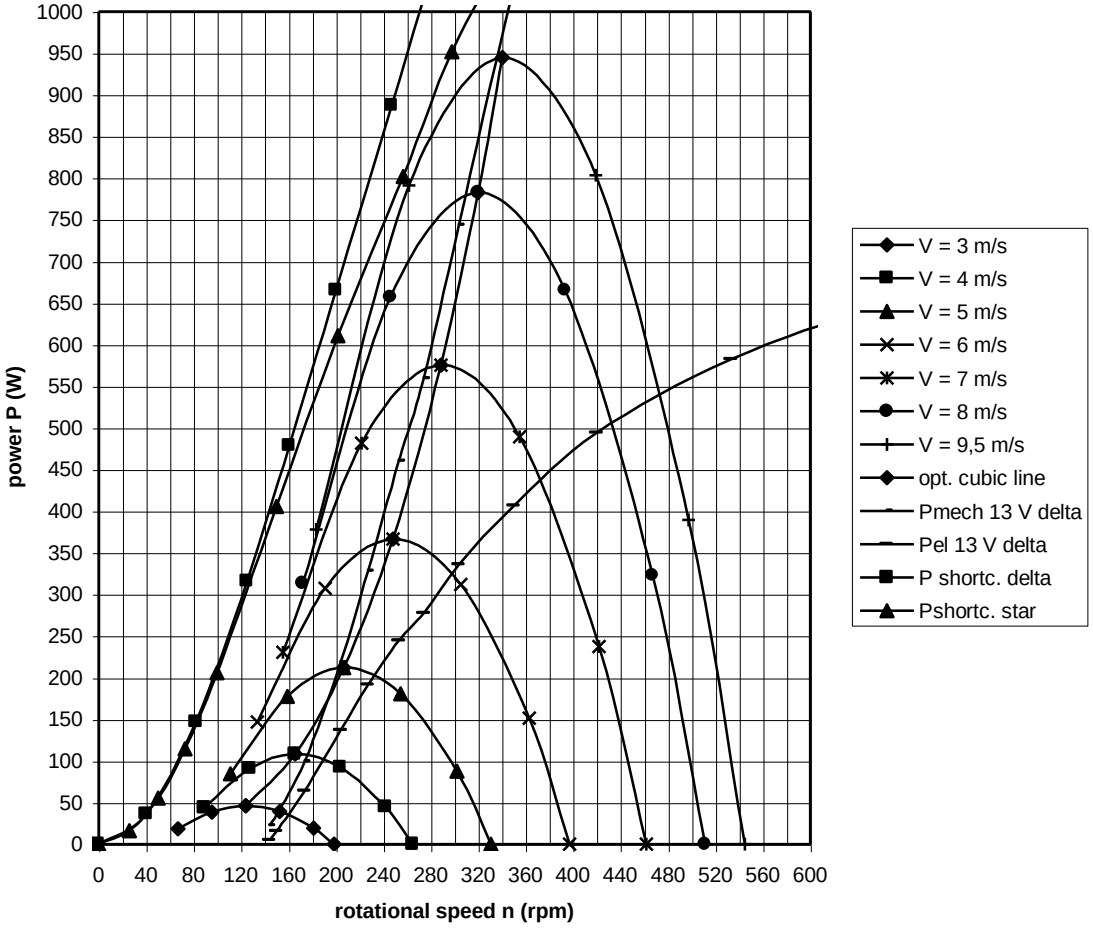

fig. 6 P-n curves of the VIRYA-3B3 rotor for V_{rated} = 9.5 m/s, optimum cubic line, P_{mech}-n and P_{el}-n curves of the generator with modified 115/200 V winding for 13 V delta and P-n curves of the generator for short-circuit in delta and star.

In figure 6 it can be seen that the matching is even better as for 26 V star. An advantage of delta rectification is that making short circuit in delta requires no extra line to the short-circuit switch and that a 2-pole short-circuit switch can be used.

The P_{el}-V curve for 13 V delta is derived from figure 6 using the method given in chapter 5. The P_{el}-V curve is given in figure 7.

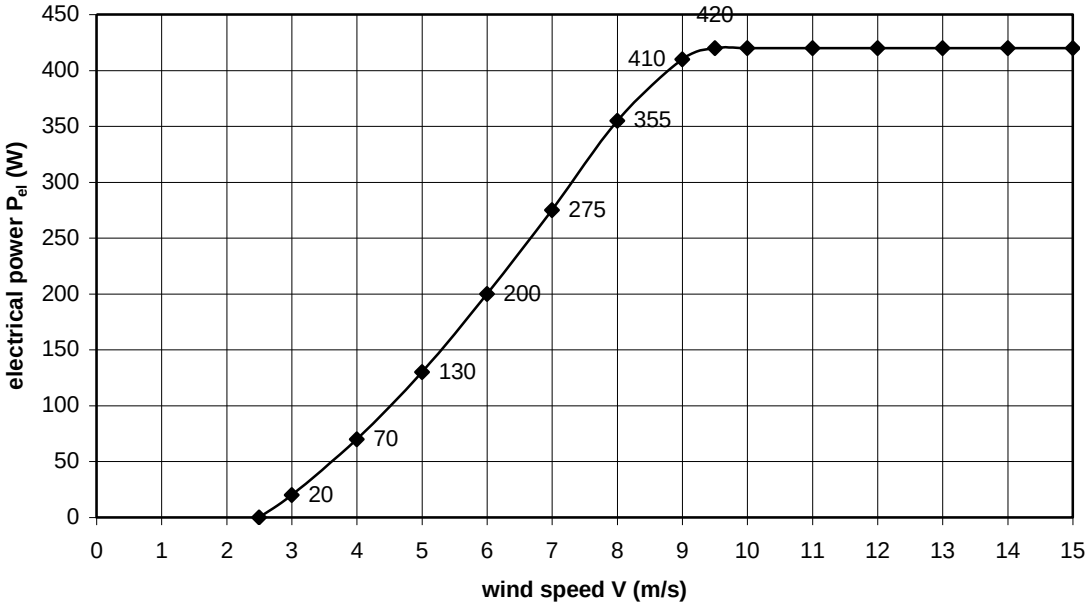

fig. 7 P_{el}-V curve of the VIRYA-3B3 windmill with V_{rated} = 9.5 m/s for 12 V battery charging and rectification of the modified 115/200 V winding in delta

In figure 7 it can be seen that the maximum power is 420 W which is 80 W lower than for 26 V star. The whole P_{el}-V curve is lying lower than for 26 V star except for wind speeds below 4 m/s. This is because of the lower generator efficiency in delta. The cut-in wind speed lies at about 2.5 m/s which is a little lower than for 26 V star.

A disadvantage of 12 V battery charging is that the charging current is rather large. If the charging voltage is 14 V and if the supplied power is 420 W, the charging current is 30 A. To limit voltage lossen in the cables in between the generator and the batteries rather thick wires have to be used.

It is possible to use the original 230/400 V winding for 24 V battery charging if the winding is rectified in delta. For this situation the same P_{el}-V curve will be found as given in figure 7. So the power will be lower as for the modified 115/200 V winding, rectified in star. Another disadvantage is that the starting behavior in delta is worse than in star because the unloaded P_{mech}-n curve of the generator is rising faster in delta than in star. This is because in delta, higher harmonic currents can circulate in the winding.

6 Checking of the starting behaviour

In chapter 4 it has been calculated that the starting wind speed is 2.7 m/s. At this wind speed the rotor is able to generate the unloaded sticking torque of 0.4 Nm of the generator if the shaft is not rotating. The unloaded sticking torque increases at increasing rotational speeds but how much depends on how the generator is rectified. The sticking torque for rectification in delta rises faster than for rectification in star because higher harmonic currents can circulate in delta. The sticking torque has been measured for both situations and the result is given in figure 1 of report KD 78 (ref. 1). These curves are copied in figure 8.

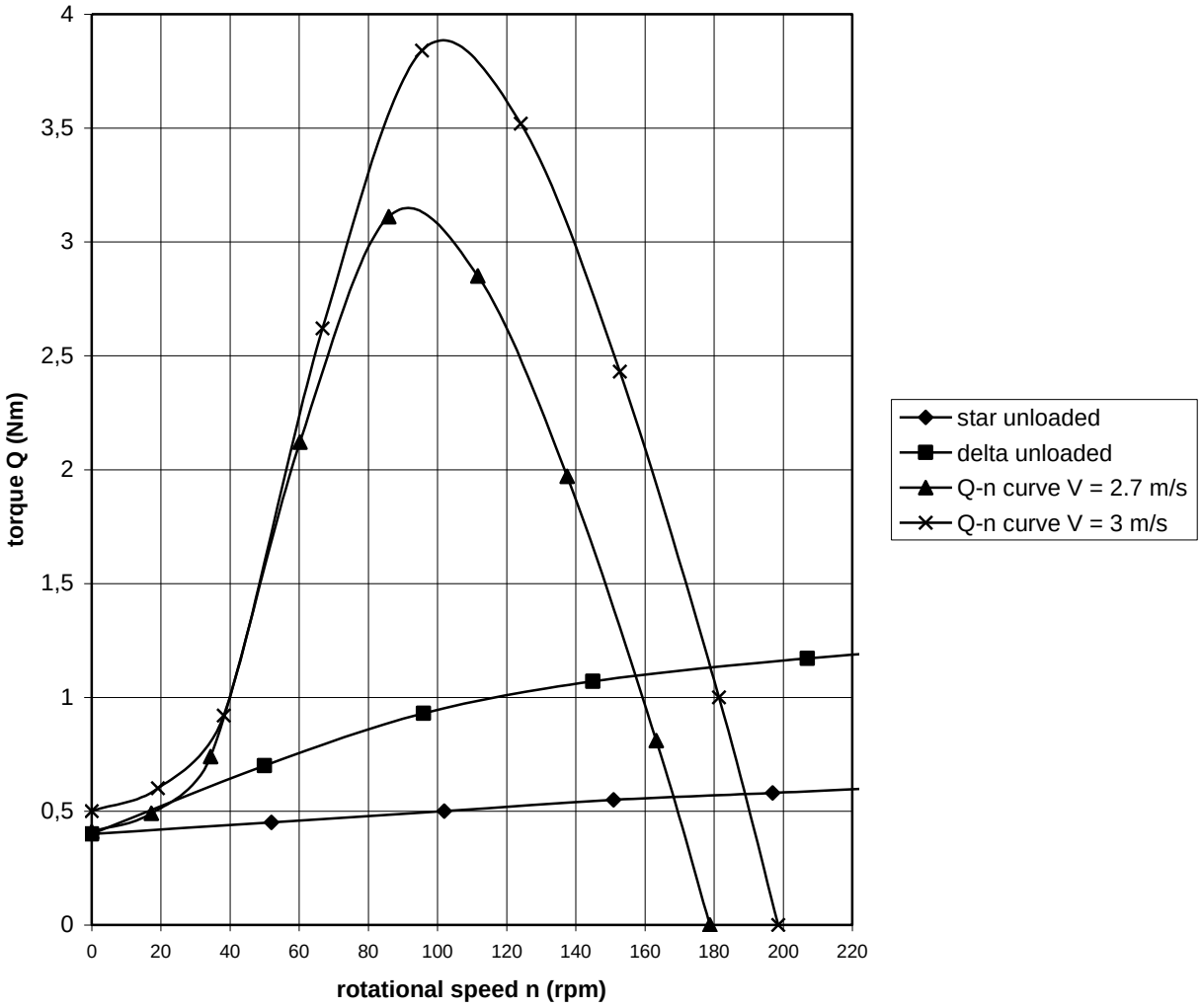

fig. 8 Unloaded sticking torque of the generator with modified 115/200 V winding for rectification in star and delta and Q-n curves of the rotor for V = 2.7 m/s and V = 3 m/s

The Q-n curve of the rotor for a certain wind speed can be determined in the same way as the P-n curve for a certain wind speed but one has to use the formula for Q in stead as the formula for P. The formula for Q for a rotor perpendicular to the wind is given by formula 4.3 of KD 35. Substitution of $\rho = 1.2$ kg/m^3 , V = 2.7 m/s and R = 1.5 m in this formula gives:

$$Q = 46.377 * C_q \quad \text{(Nm)} \qquad (10)$$

The rotational speed n is given by formula 8. Substitution of $\delta = 0°$ and V = 2.7 m/s in formula 8 gives:

$$n = 17.189 * \lambda \quad \text{(rpm)} \qquad (11)$$

The Q-n curve is now determined for values λ of 0, 1, 2, 3.5, 5, 6.5, 8, 9.5 and 10.4 and the corresponding values of C_q (see figure 2). The Q-n curve found this way is also given in figure 8. In figure 8 it can be seen that the Q-n curve for V = 2.7 m/s at low rotational speeds is rising faster than the unloaded sticking torque for rectification in star. The difference in between the Q-n curve of the rotor and the unloaded Q-n curve of the generator is used to accelerate the rotor. This means that the rotor will start at V = 2.7 m/s for rectification in star.

The Q-n curve for V = 2.7 m/s is lying below the unloaded sticking torque for rectification in delta for rotational speeds up to about 25 rpm. This means that a higher wind speed is needed to start. Assume the wind speed is 3 m/s. The Q-n curve for V = 3 m/s is determined in the same way as the curve for V = 2.7 m/s and is also drawn in figure 6. The Q-n curve for V = 3 m/s is lying higher than the unloaded Q-n curve of the rotor for delta rectification. So the rotor will start at V = 3 m/s. So the starting behaviour in delta for 13 V battery charging is acceptable but the starting behaviour in star for 24 V battery charging is better.

An advantage of delta rectification is that a 2-phase switch can be used for making short-circuit. If the generator is rectified in star one has to make short-circuit in delta and this is gained if the star point is short-circuited too. However, this requires an extra wire from the star point to the short-circuit switch and it also requires a more expensive 3-phase short-circuit switch.

8 Calculation of the strength of the hub plate

The blades are connected to each other by the hub plate. An ear of the hub plate has a length to the centre of 225 mm. The width b = 130 mm and the height h = 5 mm. The wooden blade has a width of 150 mm and a thickness of 18 mm and so the moment of resistance of the blade is much larger. It is therefore assumed that the hub plate is the weakest component.

The ear is loaded by a bending moment with axial direction which is caused by the rotor thrust and by the gyroscopic moment. The ear is also loaded by a centrifugal force and by a bending moment with tangential direction caused by the torque and by the weight of the blade but the stresses which are caused by these loads can be neglected.

Because the hub plate ear is rather thin it makes the blade connection elastic and therefore the blade will bend backwards already at a low load. As a result of this bending, a moment with direction forwards is created by a component of the centrifugal force in the blade. The bending is substantially decreased by this moment and this has a favourable influence on the bending stress.

It is started with the determination of the bending stress which is caused by the rotor thrust. There are two critical situations:

1e The load which appears for a rotating rotor at V_{rated} = 9.5 m/s. For this situation the bending stress is decreased by the centrifugal moment. The yaw angle is 30° for V_{rated} = 9.5 m/s.

2e The load which appears for a slowed down rotor. The rotor is slowed down by making short-circuit in the generator winding. A graph has been made in which the Q-n curve of the rotor for V = 9.5 m/s has been plotted together with the Q-n curve of the generator for short-circuit in delta. For the working point it is found that the rotor rotates at a rotational speed of about 13 rpm and has a tip speed ratio of about 0.2. For this very low rotational speed the effect of compensation by the centrifugal moment is negligible and a tip speed ratio of 0.2 is very low. Therefore it is assumed that the rotor stands still.

8.1 Bending stress in the strip for a rotating rotor and V = 9.5 m/s

The rotor thrust is given by formula 7.4 of KD 35. The rotor thrust is the axial load of all blades together and exerts in the hart of the rotor. The thrust per blade $F_{t\,\delta\,bl}$ is the rotor thrust $F_{t\,\delta}$ divided by the number of blades B. This gives:

$$F_{t\,\delta\,bl} = C_t * \cos^2\delta * \tfrac{1}{2}\rho V^2 * \pi R^2 / B \qquad (N) \qquad (12)$$

For the rotor theory it is assumed that every small area dA which is swept by the rotor, supplies the same amount of energy and that the generated energy is maximised. For this situation the wind speed in the rotor plane has to be slowed down till 2/3 of the undisturbed wind speed V. This results in a pressure drop over the rotor plane which is the same for every value of r. It can be proven that this results in a triangular axial load which forms the thrust and in a constant radial load which supplies the torque.

The theoretical thrust coefficient C_t for the whole rotor is 8/9 = 0.889 for the optimal tip speed ratio. In practice C_t is lower because of the tip losses and because the blade is not effective up to the rotor centre. The effective blade length k' of the VIRYA-3B3 rotor is only 1.05 m but the rotor radius R = 1.5 m. Therefore there is a disk in the centre with an area of about 0.09 of the rotor area on which almost no thrust is working. This results in a theoretical thrust coefficient $C_t = 8/9 * 0.91 = 0.809$. Because of the tip losses the real C_t value is substantially lower. Assume this results in a real practical value of $C_t = 0.7$. It is assumed that the thrust coefficient is constant for values of λ in between λ_d and $\lambda_{unloaded}$.
Substitution of $C_t = 0.7$, $\delta = 30°$, $\rho = 1.2$ kg/m^3, V = 9.5 m/s, R = 1.5 m and B = 3 in formula 12 gives $F_{t\,\delta\,bl} = 67$ N.

For a pure triangular load, the same moment is exerted in the hart of the rotor as for a point load which exerts in the centre of gravity of the triangle. The centre of gravity is laying at 2/3 R = 1 m. Because the effective blade length is only k', there is no triangular load working on the blade but a load with the shape of a trapezium as the triangular load over the part R – k' falls off. The centre of gravity of the trapezium has been determined graphically and is laying at about $r_1 = 1.05$ m.

The maximum bending stress is not caused at the hart of the rotor but at the edge of the hub because the strip bends backwards from this edge. This edge is laying at $r_2 = 0.035$ m. At this edge we find a bending moment $M_{b\,t}$ caused by the thrust which is given by:

$$M_{b\,t} = F_{t\,\delta\,bl} * (r_1 - r_2) \qquad \text{(Nm)} \qquad (13)$$

Substitution of $F_{t\,\delta\,bl} = 67$ N, $r_1 = 1.05$ m and $r_2 = 0.035$ m gives $M_{b\,t} = 68$ Nm = 68000 Nmm.

For the stress we use the unit N/mm^2 so the bending moment has to be given in Nmm. The bending stress σ_b is given by:

$$\sigma_b = M / W \qquad (N/mm^2) \qquad (14)$$

The moment of resistance W of a strip is given by:

$$W = 1/6\ bh^2 \qquad (mm^3) \qquad (15)$$

(14) + (15) gives:

$$\sigma_b = 6\ M / bh^2 \qquad (N/mm^2) \qquad (M \text{ in Nmm}) \qquad (16)$$

Substitution of M = 68000 Nmm, b = 130 mm and h = 5 mm in formula 16 gives $\sigma_b = 126$ N/mm^2. For this stress the effect of the stress reduction by bending forwards of the blade caused by the centrifugal force in the blade has not yet been taken into account. The gyroscopic moment has also not yet been taken into account.

Next it is investigated how far the blade bends backwards as a result of the thrust load and what influence this bending has on the centrifugal moment. Hereby it is assumed that the strip is only bending over part from the inner connecting bolt to the hub. The inner connecting bolt point lays at $r_3 = 0.095$ m = 95 mm.

So the length of the strip l which is loaded by bending is given by:

$$l = r_3 - r_2 \qquad (mm) \qquad (17)$$

The load from the blade on the strip at r_3 can be replaced by a moment M and a point load F. F is equal to $F_{t\,\delta\,bl}$. M is given by:

$$M = F * (r_1 - r_3) \qquad (Nmm) \qquad (18)$$

The bending angle ϕ (in radians) at r_3 for a strip with a length l is given by (combination of the standard formulas for a moment plus a point load):

$$\phi = l * (M + \tfrac{1}{2} Fl) / EI \qquad (rad) \qquad (19)$$

The bending moment of inertia I of a strip is given by:

$$I = 1/12\ bh^3 \qquad (mm^4) \qquad (20)$$

(17) + (18) + (19) + (20) gives:

$$\phi = 12 * F * (r_3 - r_2) * \{(r_1 - r_3) + \tfrac{1}{2} (r_3 - r_2)\} / (E * bh^3) \qquad (rad) \qquad (21)$$

Substitution of F = 67 N, r_3 = 95 mm, r_2 = 35 mm, r_1 = 1050 mm, E = 2.1 * 10^5 N/mm^2, b = 130 mm and h = 5 mm in formula 21 gives: ϕ = 0.01392 rad = 0.80°. This is an angle which can not be neglected. In report R409D (ref. 7) a formula is derived for the angle ε with which the blade moves backwards if it is connected to the hub by a hinge. This formula is valid if both the axial load and the centrifugal load are triangular. For the VIRYA-3B3 this is not exactly the case but the formula gives a good approximation. The formula is given by:

$$\varepsilon = \arcsin\left(\frac{C_t * \rho * R^2 * \pi}{B * A_{pr} * \rho_{pr} * \lambda^2}\right) \qquad (°) \qquad (22)$$

In this formula A_{pr} is the cross sectional area of the airfoil (in m^2) and ρ_{pr} is the density of the used airfoil material (in kg/m^3). The average thickness of a Gö 623 airfoil is about a factor 0.7 of the maximum thickness. So the cross sectional area is 0.7 * 18 * 150 = 1890 mm^2 = 0.00189 m^2. The blade is made of hard wood with a density ρ_{pr} of about ρ_{pr} = 0.6 * 10^3 kg/m^3. In figure 4 it can be seen that for high wind speeds, the rotor is running at about λ = 6.8. Substitution of C_t = 0.7, ρ = 1.2 kg/m^3, R = 2 m, B = 3, A_{pr} = 0.00189 m^2, ρ_{pr} = 0.6 * 10^3 kg/m^3 and λ = 6.8 in formula 22 gives: ε = 2.16°. This angle is larger than the calculated angle of 0.8° with which the blade would bend backwards if the compensating effect of the centrifugal moment is not taken into account. This means that the real bending angle will be less than 0.8°.

The real bending angle ε is determined a follows. A thrust moment M_t = 68 Nm is working backwards and M_t is independent of ε for small values of ε. A bending moment M_b is working forwards and M_b is proportional with ε. M_b = 68 Nm for ε = 0.8°. A centrifugal moment M_c is working forwards and M_c is also proportional with ε. M_c = 68 Nm for ε = 2.16°. The path of these three moments is given in figure 9. The sum total of M_b + M_c is determined and the line M_b + M_c is also given in figure 9.

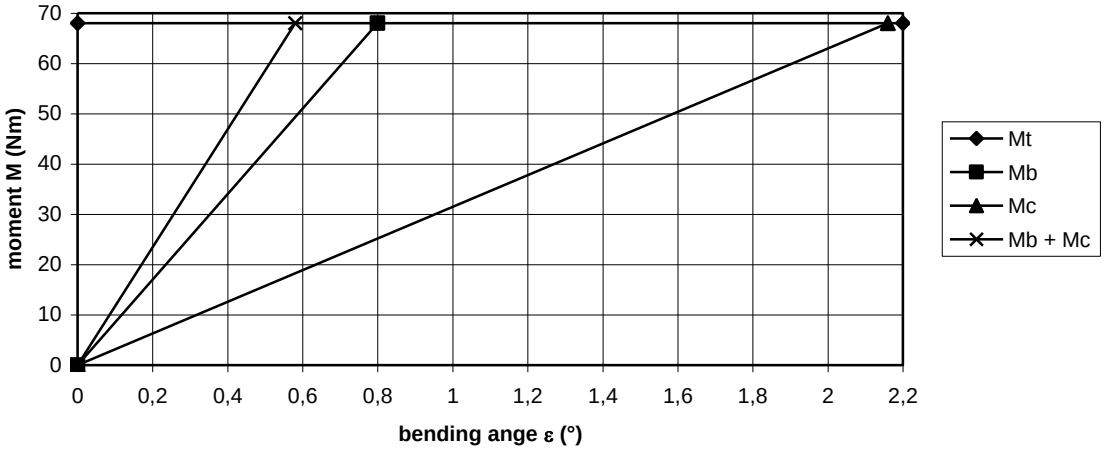

fig. 9 Path of M_t, M_b, M_c, and $M_b + M_c$ as a function of ε

The point of intersection of the line of M_t with the line of $M_b + M_c$ gives the final angle ε. In figure 9 it can be seen that ε = 0.58°. This is a factor 0.725 of the calculated angle of 0.8°. Because the bending stress is proportional to the bending angle it will also be a factor 0.725 of the calculated stress of 126 N/mm^2 resulting in a stress of about 91 N/mm^2. This is a rather low stress but up to now the gyroscopic moment, which can be rather large, has not yet been taken into account.

The gyroscopic moment is caused by simultaneously rotation of rotor and head. One can distinguish the gyroscopic moment in a blade and the gyroscopic moment which is exerted by the whole rotor on the rotor shaft and so on the head. On a rotating mass element dm at a radius r, a gyroscopic force dF is working which is maximum if the blade is vertical and zero if the blade is horizontal and which varies with sinα with respect to a rotating axis frame. α is the angle with the blade axis and the horizon. So it is valid that $dF = dF_{max} * \sin\alpha$. The direction of dF depends on the direction of rotation of both axis and dF is working forwards or backwards. The moment dF * r which is exerted by this force with respect to the blade is therefore varying sinusoidal too.

However, if the moment is determined with respect to a fixed axis frame it can be proven that it varies with $dF_{max} * r \sin^2\alpha$ with respect to the horizontal x-axis and with $dF_{max} * \sin\alpha * \cos\alpha$ with respect to the vertical y-axis. For two and more bladed rotors it can be proven that the resulting moment of all mass elements around the y-axis is zero.

For a single blade and for two bladed rotors, the resulting moment of all mass elements with respect to the x-axis is varying with $\sin^2\alpha$, so just the same as for a single mass element. However, for three and more bladed rotors, the resulting moment of all mass elements with respect to the x-axis is constant. The resulting moment with respect to the x-axis for a three (or more) bladed rotor is given by the formula:

$$M_{gyr\ x\text{-}as} = I_{rot} * \Omega_{rot} * \Omega_{head} \qquad \text{(Nm)} \qquad (23)$$

In this formula I_{rot} is the mass moment of inertia of the whole rotor, Ω_{rot} is the angular velocity of the rotor and Ω_{head} is the angular velocity of the head. The resulting moment is constant for a three bladed rotor because adding three $\sin^2\alpha$ functions which make an angle of 120° which each other, appear to result in a constant value. The three functions are given in figure 10. It can be proven for a three bladed rotor that the sum value of the three blades is equal to 3/2 of the peak value of one blade.

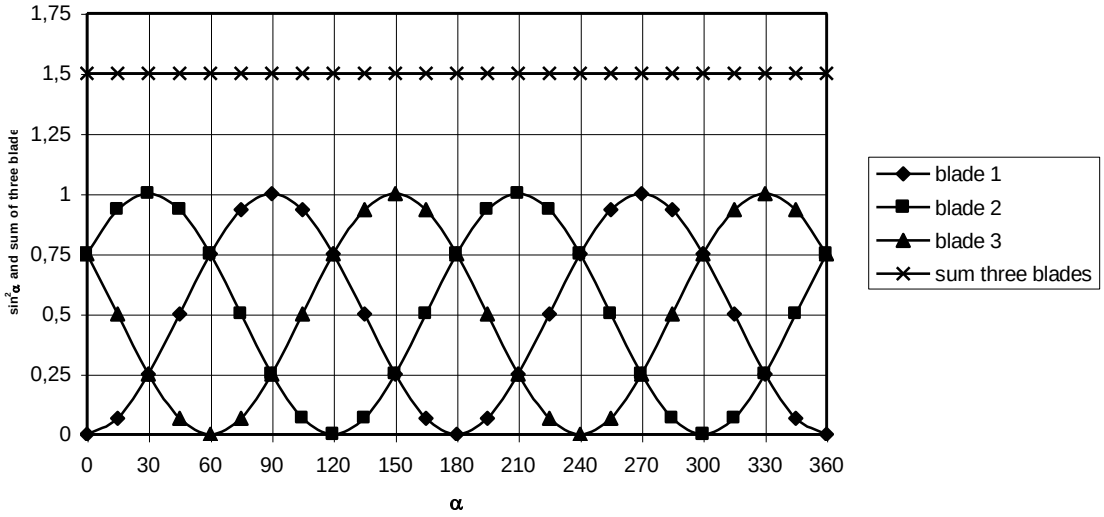

fig. 10 Path of $\sin^2\alpha$ and the sum of three blades

For the calculation of the blade strength we are not interested in the variation of the gyroscopic moment with respect to a fixed axis frame but in variation of the moment in the blade itself so with respect to a rotation axis frame for which it was explained earlier that the moment is varying sinusoidal. If the blade is vertical both axis frames coincide and the moment for both axis frames is the same. The maximum moment in one blade is then 2/3 of the sum moment as given by formula 23. The variation of the moment in the blade with respect to a rotating axis frame is therefore given by:

$$M_{gyr\,bl} = 2/3 \sin\alpha * I_{rot} * \Omega_{rot} * \Omega_{head} \qquad \text{(Nm)} \qquad (24)$$

For a three bladed rotor, the moment of inertia of the whole rotor I_{rot} is three times the moment of inertia of one blade I_{bl}. Therefore it is valid that:

$$M_{gyr\,bl} = 2 \sin\alpha * I_{bl} * \Omega_{rot} * \Omega_{head} \qquad \text{(Nm)} \qquad (25)$$

Up to now it is assumed that the blades have an infinitive stiffness. However, in reality the blades are flexible and will bend by the fluctuations of the gyroscopic moment. Therefore the blade will not follow the curve for which formula 24 and 25 are valid. I am not able to describe this effect physically but the practical result of it is that the strong fluctuation on the $\sin^2\alpha$ function is rather flattened. However, the average moment is assumed to stay the same as given by formula 21. I estimate that the flattened peak value is given by:

$$M_{gyr\,bl\,max} = 1.2 * I_{bl} * \Omega_{rot} * \Omega_{head} \qquad \text{(Nm)} \qquad (26)$$

For the chosen blade geometry it is calculated that $I_{bl} = 1.28$ kgm^2. The maximum loaded rotational speed of the rotor can be read in figure 4 and it is found that $n_{max} = 360$ rpm. This gives $\Omega_{rot\,max} = 37.7$ rad/s (because $\Omega = \pi * n / 30$).

It is not easy to determine the maximum yawing speed. The VIRYA-3B3 is provided with the hinged side vane safety system which has a light van blade and a large moment of inertia of the whole head around the tower axis. This is because the vane arm is a part of the head. For sudden variations in wind speed and wind direction the vane blade will therefore react very fast but the head will follow only slowly. It is assumed that the maximum angular velocity of the head can be 0.3 rad/s at very high wind speeds.

Substitution of I_{bl} = 1.28 kgm^2, $\Omega_{rot\ max}$ = 37.7 rad/s en $\Omega_{head\ max}$ = 0.3 rad/s in formula 24 gives: $M_{gyr\ bl\ max}$ = 17.4 Nm = 17400 Nmm.
Substitution of M = 17400 Nmm, b = 130 mm and h = 5 mm in formula 14 gives $\sigma_{b\ max}$ = 32 N/mm^2. This value has to be added to the bending stress of 91 N/mm^2 which was the result of the thrust because there is always a position were both moments are strengthening each other. This gives $\sigma_{b\ tot\ max}$ = 123 N/mm^2. The minimum stress is 91 - 32 = 59 N/mm^2. So the stress is not becoming negative and therefore it is not necessary to take the load as a fatigue load.

For the strip material stainless steel AISI 304 (MCB quality 1.4301) is chosen. The 0.2 % deformation limit for this steel is 230 N/mm^2. However this is for a pulling stress. The deformation limit for a bending stress is much higher and it is expected that it is 350 N/mm^2. The allowable fatigue stress is much lower than the 0.2 % deformation stress for bending because stainless steel is sensible to fatigue. The value is not given in the MCB catalogue but it is assumed that the allowable fatigue stress for bending is half the 0.2 % deformation limit for bending, so 175 N/mm^2. It is assumed that the allowable bending stress for a non fatigue stress is 230 N/mm^2. The calculated stress is even lower than the allowable fatigue stress so the strip is strong enough.

In reality the blade is not extremely stiff and will also bend somewhat. This reduces the bending of the strip and therefore the stress is the strip will be somewhat lower.

8.2 Bending stress in the strip for a slowed down rotor

The rotational speed for a rotor which is slowed down by making short-circuit of the generator is very low. Therefore there is no compensating effect of the centrifugal moment on the moment of the thrust. However, there is also no gyroscopic moment. The safety system is also working if the rotor is slowed down but a much larger wind speed will be required to generate the same thrust as for a rotating rotor.

In chapter 6.1 it has been calculated that the maximum thrust on one blade for a rotating rotor is 67 N for V = V_{rated} = 9.5 m/s and δ = 30°. The head turns out of the wind such at higher wind speeds, that the thrust stays almost constant above V_{rated}. A slowed down rotor will therefore also turn out of the wind by 30° if the force on one blade is 67 N. Also for a slowed down rotor the force is staying constant for higher yaw angles. However, for a slowed down rotor, the resulting force of the blade load is exerting in the middle of the blade at r_4 = 0.75 m because the relative wind speed is almost constant along the whole blade. The bending moment around the edge of the hub is therefore somewhat smaller. Formula 13 changes into:

$$M_{b\,t} = F_{t\,\delta\,bl} * (r_4 - r_2) \qquad \text{(Nm)} \qquad (27)$$

Substitution of $F_{t\,\delta\,bl}$ = 67 N, r_4 = 0.75 m en r_2 = 0.035 m in formula 27 gives $M_{b\,t}$ = 48 Nm = 48000Nmm. Substitution of M = 48000 Nmm, b = 130 mm and h = 5 mm in formula 16 gives σ_b = 89 N/mm^2. This is lower than the calculated stress for a rotating rotor. The load is not fluctuating and therefore it is surly not necessary to use the allowable fatigue stress. The allowable stress is 230 N/mm^2, so the strip is strong enough.

Because the strip and the blade are rather flexible it has to be checked if a slowed down rotor can't hit the tower. In chapter 6.1 it has been calculated, for no compensation of the gyroscopic moment, that the bending angle is 0.8° for a stress of 126 N/mm^2. So for a stress of 89 N/mm^2 the bending angle will be 0.8 * 89 / 126 = 0.57°. For a rotor radius of R = 1.5 m this results in a movement at the tip of about 0.015 m. Because the blade itself will bend too, the movement will be larger and it is expected that it will be about 0.03 m. The minimum distance in between the blade tip and the tower pipe is much larger if the blade is not bending. So there is no chance that the blade hits the tower for a slowed down rotor.

9 References

1 Kragten A. Measurements performed on a generator with housing 5RN90L04V and a 4-pole armature equipped with neodymium magnets, March 2001, reviewed March 2015, free public report KD 78, engineering office Kragten Design, Populierenlaan 51, 5492 SG Sint-Oedenrode, The Netherlands.

2 Kragten A. Rotor design and matching for horizontal axis wind turbines, January 1999, reviewed February 2017, free public rapport KD 35, engineering office Kragten Design, Populierenlaan 51, 5492 SG Sint-Oedenrode, The Netherlands.

3 Kragten A. Determination of C_q for low values of λ. Deriving the C_p-λ and C_q-λ curves of the VIRYA-1.8D rotor, July 2002, free public rapport KD 97, engineering office Kragten Design, Populierenlaan 51, 5492 SG Sint-Oedenrode, The Netherlands.

4 Kragten A. Method to check the estimated δ-V curve of the hinged side vane safety system and checking of the δ-V curve of the VIRYA-4.2 windmill, December 2004, free public report KD 213, engineering office Kragten Design, Populierenlaan 51, 5492 SG Sint-Oedenrode.

5 Kragten A. Development of the permanent magnet (PM) generators of the VIRYA windmills, May 2007, reviewed December 2017, free public report KD 341,¶ engineering office Kragten Design, Populierenlaan 51, 5492 SG Sint-Oedenrode, The Netherlands.

6 Kragten A. Rectification of 3-phase VIRYA windmill generators, May 2007, reviewed October 2014, free public report KD 340, engineering office Kragten Design, Populierenlaan 51, 5492 SG Sint-Oedenrode.

7 Kragten A. Bepaling kegelhoek ε en de grootte van de centrifugaalgewichten voor snellopende propellers, in Dutch, July 1980, report R 409 D, University of Technology Eindhoven, Faculty of Physics, Laboratory of Fluid Dynamics and Heat Transfer, P.O. box 513, 5600 MB Eindhoven, The Netherlands, (report probably no longer available).

10 Appendix 1 Sketch of the VIRYA-3B3 rotor

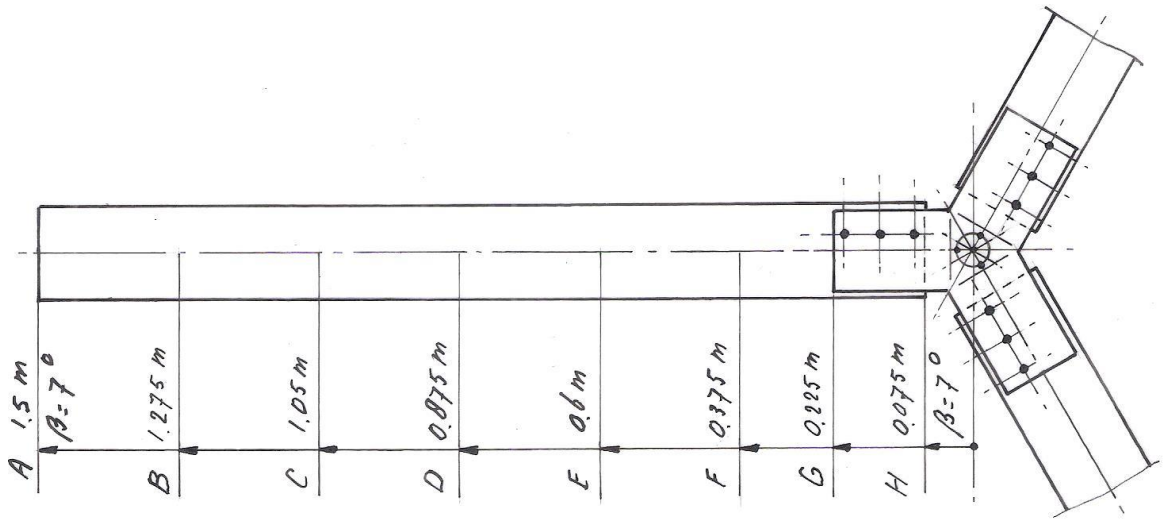

11 Appendix 2 Photo drawing VIRYA-3B3 rotor